

This work was written as part of one of the author's official duties as an Employee of the United States Government and is therefore a work of the United States Government. In accordance with 17 U.S.C. 105, no copyright protection is available for such works under U.S. Law.

Public Domain Mark 1.0

<https://creativecommons.org/publicdomain/mark/1.0/>

Access to this work was provided by the University of Maryland, Baltimore County (UMBC) ScholarWorks@UMBC digital repository on the Maryland Shared Open Access (MD-SOAR) platform.

Please provide feedback

Please support the ScholarWorks@UMBC repository by emailing scholarworks-group@umbc.edu and telling us what having access to this work means to you and why it's important to you. Thank you.

Origin and dynamics of the heliospheric streamer belt and current sheet

D. Aaron Roberts

NASA Goddard Space Flight Center, Laboratory for Solar and Space Physics, Greenbelt, Maryland, USA

Paul A. Keiter¹

Department of Physics, West Virginia University, Morgantown, West Virginia, USA

Melvyn L. Goldstein

NASA Goddard Space Flight Center, Laboratory for Solar and Space Physics, Greenbelt, Maryland, USA

Received 15 April 2004; revised 8 March 2005; accepted 22 March 2005; published 11 June 2005.

[1] The broad high-density, low-temperature region around the thin heliospheric current sheet at solar minimum forms a relatively stable “streamer belt” associated with the slow wind flow. This region contains highly structured magnetic fields, with large rotations and discontinuities being common. This observational study examines the likely origins and dynamics of the interplanetary plasma and current sheets primarily using Helios data. The striking differences sometimes observed between the plasma on the two sides of the current sheet support the common interpretation that the plasma above and below the sheet comes from often very different regions located either side of the helmet streamer at the base of the slow wind flow. The entropy per proton in the streamer belt often shows sharply defined regions of strongly different plasma; this implies that the origin of the filamentary structure is in initial conditions near the Sun because dynamical evolution can only equalize entropy. The observed large relative density and other fluctuations may thus represent the conditions on flow tubes with different boundary conditions. The average entropy in the streamer belt increases by about the same factor as in the surrounding high-speed streams, indicating that this region is heated substantially, consistent with studies of the temperature evolution and with turbulence modeling. Compressive stream interaction regions are not preferentially heated (in the sense of an entropy increase) in the inner heliosphere. Strong anticorrelations between density and both temperature and magnetic field magnitude are observed within the streamer belt but not in the surrounding regions, and these become weaker as the flow moves outward. Both the smoother appearance of the entropy at greater heliocentric distance and simulation evidence support the view that the streamer belt region undergoes significant dynamical evolution. This evolution seems to also affect the current sheet because sector boundary crossings are observed to become more complex (more multiple crossings) with increasing heliocentric distance. The crossings are more complex in general near solar maximum, although the complexity still increases with radial distance.

Citation: Roberts, D. A., P. A. Keiter, and M. L. Goldstein (2005), Origin and dynamics of the heliospheric streamer belt and current sheet, *J. Geophys. Res.*, 110, A06102, doi:10.1029/2004JA010541.

1. Introduction

[2] When the Sun is least active, dominant polar coronal holes give rise to high-speed streams above and below the heliographic equator. In between, in a region surrounding the heliospheric magnetic sector boundary and radially outward from a large helmet streamer, lies a dense, cool,

slower-flowing plasma. As in the case of the Earth’s magnetotail, it is the flow of the wind stretching the basically dipolar field of the source regions that leads to a current sheet in the equatorial region separating hemispheres of opposite magnetic polarity, and thus it is reasonable to term the dense equatorial plasma a “plasma sheet” in the solar case. However, since this term is sometimes used for very small regions within the region of interest here [Winterhalter *et al.*, 1994], we will refer to the slow, high-density region as the “streamer belt” in accordance with the usage of Gosling *et al.* [1981] and consistent with the many studies supporting the idea that the broad plasma sheet is an

¹Now at Los Alamos National Laboratory, Los Alamos, New Mexico, USA.

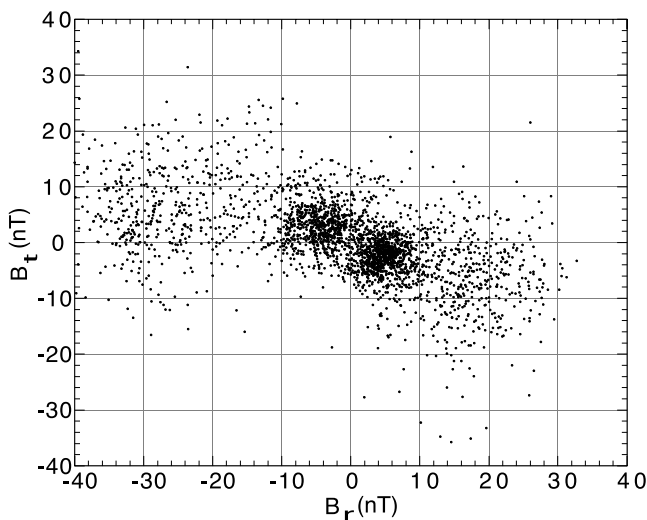


Figure 1. Data from Helios 2 1976 plotting the tangential magnetic field component versus the radial magnetic field component. Most of the points are contained within two sectors, suggesting B_R can be used to locate transitions across the current sheet.

extension of the solar streamer belt [see, e.g., *Bavassano et al.*, 1997]. At solar maximum the situation becomes more complex, but regions of opposite magnetic polarity are still clear, although typically more complex than at solar minimum. This paper will examine various aspects of the current sheet and streamer belt region, using data from the inner heliosphere to complement previous studies on its origin, structure, and dynamics.

[3] It has long been known that the heliospheric streamer belt has a complex magnetic structure, with filamentary fields and strong rotations leading to a complex transition from one sector to the other in which the field magnitude often changes only slightly, and thus the current sheet is not a simple neutral sheet (see the comprehensive review by *Smith* [2001]). In addition to the magnetic complexity, the plasma properties are unusual, consisting in part of filamentary, nearly pressure balanced structures. The details of these structures at 1 AU have been studied in great detail. Crooker and coworkers [e.g., *Crooker et al.*, 1996; *Crooker*, 1999; *Crooker*, 2003] have shown that at least some of the structures are consistent with highly complex field geometries, perhaps originating at the Sun, and probably due to transient ejecta. *Szabo et al.* [1999] argued that the prevalence of these types of complexities is less than claimed by Crooker et al., and they concluded that warped fields near the current sheet accounted for many of the observations. In related simulation work, *Roberts et al.* [2003] showed that quite simple boundary conditions on the fields, combined with a modest level of wave activity, can lead to complex loops that may or may not return to the Sun on either side of the current sheet; the loops correspond well to the current sheet crossings without null lines documented in Smith's review and elsewhere. The present work will not directly address the issue of the nature of the magnetic complexity, but it will shed some light on the extent to which aspects of the structure are convected out and which are generated in the flow.

[4] Data from the outer heliosphere show that the magnetic complexity becomes greater with distance, such that the sector pattern becomes substantially different from that at 1 AU by ~ 25 AU from the Sun [*Burlaga and Ness*, 1993], evolving with distance along the way [*Behannon et al.*, 1989]. The sector pattern becomes unrelated to that seen at 1 AU at great distances from the Sun (~ 80 AU), especially toward solar maximum [*Burlaga et al.*, 2003]. The latter workers conjecture that the increase in complexity is due to stream interactions and transient solar events, and while these are certainly important aspects of the evolution, we will show here that evolution occurs even in relatively undisturbed times and in the inner heliosphere. Related earlier work by *Thieme et al.* [1990] showed that high-speed streams at solar minimum contain signatures of varied coronal conditions on different flow tubes that become less evident with increasing heliocentric distance; we will demonstrate that both the striation and dynamical evolution are more striking for the streamer belt. There is earlier evidence for this type of evolution in the slow wind within 0.3 AU by *Woo et al.* [1995], who compared radio scintillation measurements near the Sun with in situ measurements beyond 0.3 AU. Our approach to these and other questions will be to follow solar wind plasma from 0.3 to 1 AU using recurrent streams and statistical analysis of large data collections.

2. Data Sets and Analysis Procedure

[5] We use hour-averaged data covering 0.3 to 1.0 AU from Helios 1 spanning the years of 1975–1980 and from Helios 2 spanning the years 1975–1979. We also use hourly averages of Ulysses data to illustrate one point. All the data come from the “COHOWeb” data sets compiled by J. King at the National Space Science Data Center (NSSDC).

[6] We examined the complexity of heliospheric current sheet (HCS) crossings and the nature of the streamer belt at different distances from the Sun and as a function of solar cycle. Figure 1 shows a typical plot of the heliographic radial magnetic field, B_R , versus the tangential field, B_T , using data from Helios 2, 1976. This figure includes data from 0.3 to 1 AU and shows that approximately 96% of the data points clearly lie within two separate regions (sectors) and thus using B_R is a reliable way to determine where the sectors lie. Approximately 2% of the data are ambiguous. Depending on the tilt of the HCS that is considered, these points may or may not lie within a sector. Another 2% of the data are likely to be improperly identified using this method by comparison with a method using the nominal Parker spiral to determine sector identity, but this will not affect our statistics significantly. In the analysis below, we normalize the radial field by the magnitude of the field to eliminate the radial variation and make the display clearer.

[7] We initially tried to do our analysis using the azimuthal angle of the field to look for transitions, but we found that due to the periodicity of this variable, there were many times when modest changes crossing 2π radians could not be distinguished from rapid changes in the other angular direction. There are times when the angle method is superior to using the radial field, but both have difficulties. The radial field measure will change in ways that the angle will not, decreasing, for example, when the normal field com-

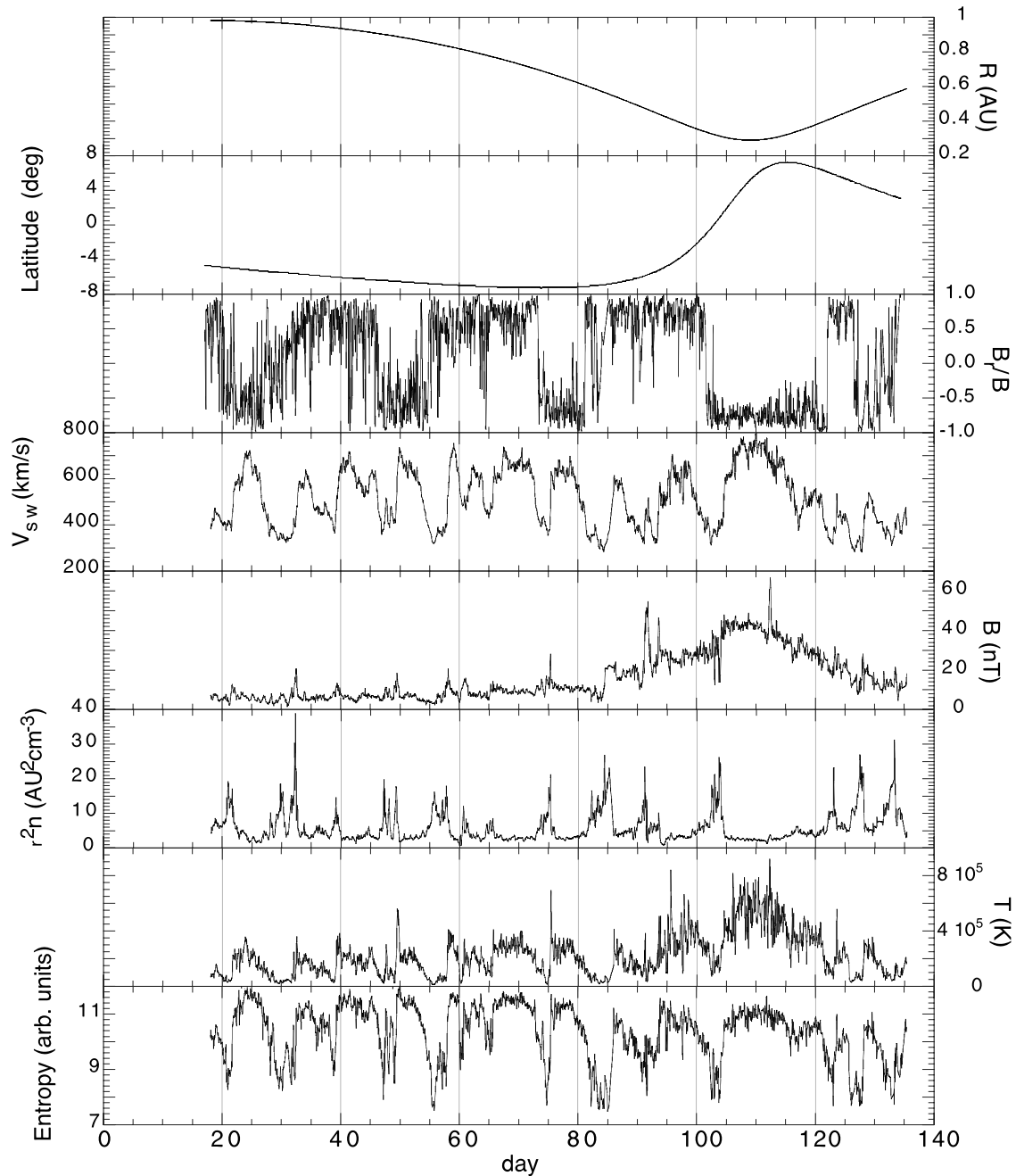


Figure 2. Data from Helios 2, 1976. From top to bottom the panels are spacecraft distance from the Sun, heliographic latitude, normalized B_R (but positive toward the Sun), magnitude of solar wind speed, magnitude of magnetic field, normalized density, temperature, and entropy.

ponent becomes large. However, smaller values do not affect changes in sign, so this will not qualitatively change the analysis. The normalized radial field also yields a measure of the sector structure that changes with radial distance, in that the typical value varies from above 0.8 at 0.3 AU to near 0.7 at 1 AU due to the change in the typical spiral field angle. This, again, is not significant in that crossings will still appear as sign changes, although with a somewhat smaller value for B_R/B either side of the crossing. Our tests have shown that the errors introduced by using the radial field are not significant, so we have used it for convenience. Note also that the angle of the spiral field is

not the same as the tilt of the current sheet and that it has nothing to do with the sheet thickness or complexity.

[8] We call distances less than 0.5 AU the “near region” and distances outside 0.5 AU the “far region.” Transitions are classified as either simple or complex. When the sign of the normalized radial component of the magnetic field reverses, the transition is considered simple if the transition happens within 5 hours and there are three or fewer crossings in the event. The transition is considered complex if it takes longer than this and has more than three crossings during the transition. These two classes cover essentially all cases observed, and, as shown below, it is usually obvious

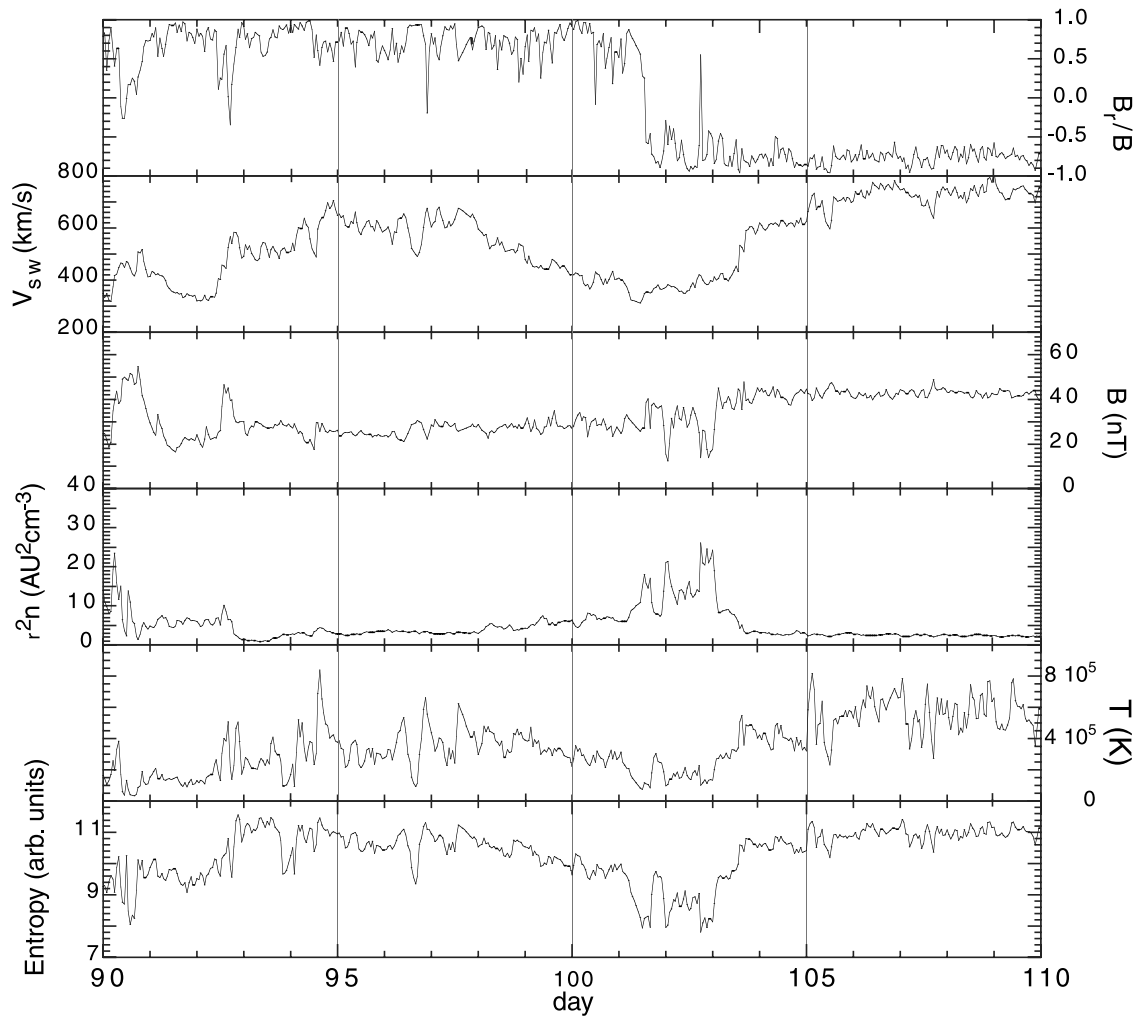


Figure 3. An enlargement of the HCS crossing around day 103. The normalized density is anticorrelated with both the magnetic field and the temperature at this transition.

to the eye which category is appropriate. We neglect the question of the nature of the complexity and of whether or not the field reversals are “true” HCS crossings and just ask the question of how the complexity as we define it depends on distance and other parameters. Increasing complexity with increased radial distance favors a view of the dynamical warping of the HCS region, whereas complexity seen close to the Sun favors a more solar origin of the features. We will find evidence for both types of signatures.

[9] As shown, for example, by *Crooker et al.* [1996], the entropy of the solar wind plasma is a good indicator of structure and processing. Differences in the entropy across a region indicate that density and temperature are to some degree anticorrelated, and thus subregions in the flow probably came from physically distinct solar sources because dynamical changes will usually change N and T simultaneously in the same direction through compression and rarefaction, leaving the entropy unchanged. We use $S = \ln(P/p^{5/3})$ to measure entropy, assuming an ideal gas law. For simplicity, we use a relative but consistent measure of entropy $S = \ln(T/N^{2/3})$, where N and T are the directly measured (not scaled) density and temperature of the protons. In the solar wind, the major obvious source of entropy production is shocks, which are easy to identify and

not generally present in the inner heliospheric intervals we consider here. We will also show evidence, consistent with previous studies, of a general irreversible heating of the plasma, perhaps by turbulence.

3. Analysis and Discussion

[10] Figure 2 shows data taken from the primary mission (1976) of Helios 2 that illustrates most of the main points. As expected at solar minimum, the HCS transitions all occur in the regions of slow speed and high density, identified with the streamer belt, that are surrounded by high-speed, low-density regions typically associated with coronal holes. Using the criteria stated above to classify HCS crossings, simple crossings are located near days 73, 82, 102, and 123. Complex crossings are located near days 20, 30, 46, and 57. There is a clear progression in B_R/B from simple transitions close to the Sun (days 102–123) and the more complex transitions occur farther from the Sun (days 20–40). (Note that B_R is positive toward the Sun due to the use of an SSE coordinate system.) Of the simple transitions, only one of them occurs when the spacecraft is rapidly changing its latitude. This case illustrates the typical picture. Of the complete set of crossings from the all of the Helios

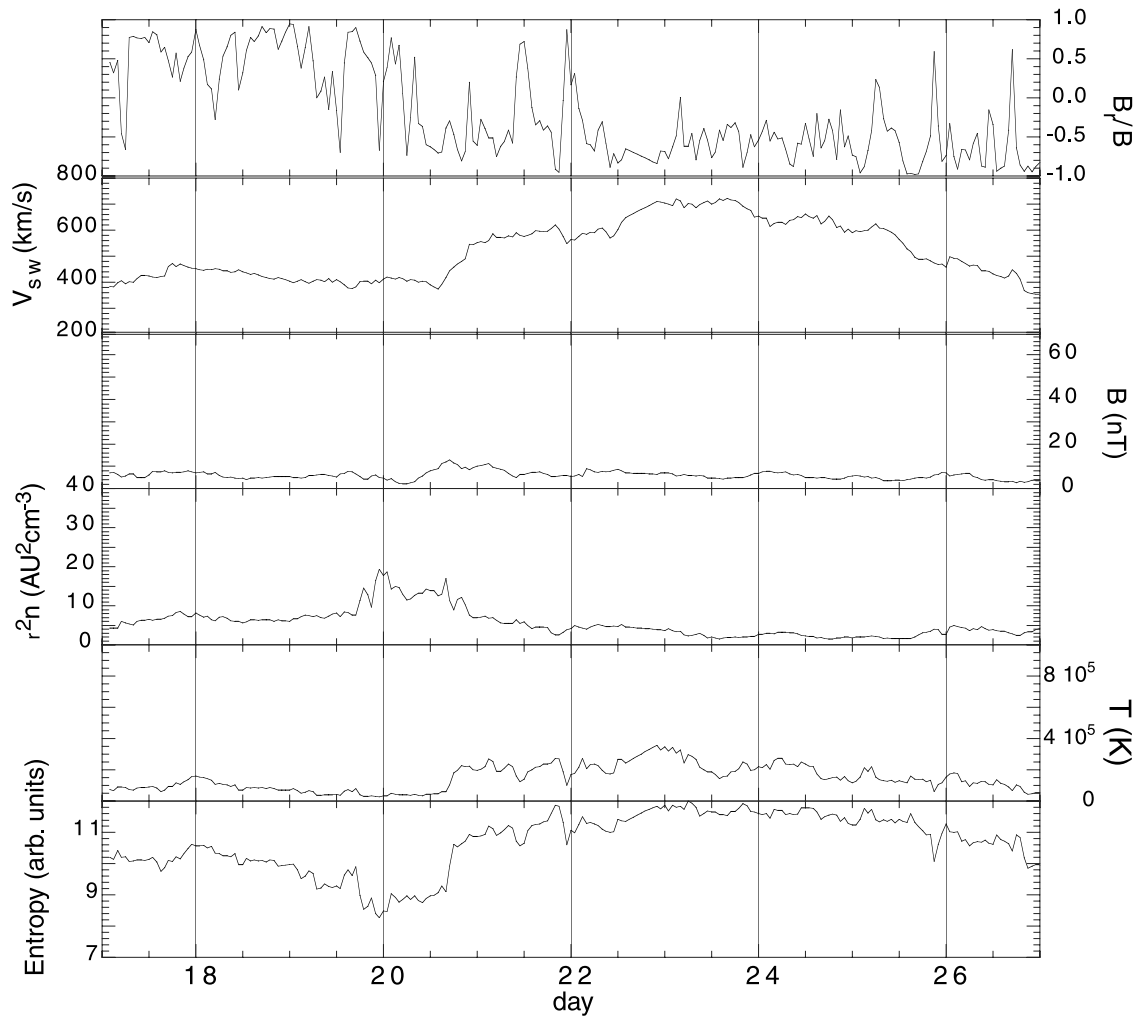


Figure 4. An enlargement of the HCS crossing of the previous figure as it appeared around day 20 when the spacecraft was near 1 AU.

data, approximately 63% have simple transitions in the near region and only 22% have simple transitions in the far region. This supports the idea that the current sheet becomes dynamically distorted as the solar wind moves away from the Sun.

[11] Next, we examine a particular corotating region seen near 1 AU around day 20 in Figure 2 and near 0.3 AU around day 101.5. Expanded plots of these regions are shown in Figures 3 and 4. This region still shows a simple transition at 0.6 AU on day 72 and it has become more complex by 0.85 AU near day 46. Thus a particular corotating region illustrates the general evolution. Figures 5 and 6 show a different view of the magnetic structure with three-dimensional (3-D) magnetic vectors projected onto the ecliptic plane. The Java-based 3-D visualization program used to make these figures is the Visual System for Browsing, Analysis, and Retrieval of Data (ViSBARD) developed by NASA and that is freely available (http://nssdcftp.gsfc.nasa.gov/selected_software/visbard/). The figures show essentially a spatial picture based on a kinematic projection of the spacecraft positions. Each actual position was changed by $\mathbf{V}_{sw}\delta t$ based on the measured solar wind speed and the time from the point of observation to a reference time. Note that this simple procedure ignores the

evolution of the fields (and can artificially project back past the Sun), but it gives a good local picture of the structures in the highly supersonic, superAlfvénic wind. The projected spacecraft positions are indicated by a symbol (“glyph”) that in this case is sized according to wind speed, which varies relatively little here, and colored according to the density. The curvature of the glyph sequence is due to the motion of the spacecraft along its orbit that makes more recently observed points lead those observed earlier.

[12] Figure 5 shows the simple, near region transition. Note that the fields become more tangential near the transition as they begin to rotate through the sector boundary, and that the reversal of the field takes place in less than an hour (the spacing between the glyphs). The region of high density persists for some hours thereafter, with a max (red glyph) in another region of nearly tangential field. The region near 1 AU, in Figure 6, also has more tangential fields near the transition region, but the transition itself now occurs over a number of hours during which the field is more complex. We do not have access to heat flux data, but that could be used to determine more of the details of the structure of the transition [see, e.g., Crooker, 1999, 2003]. Closer to the Sun in Figure 6, the density again has a second peak (light green glyph), although now not the largest, and

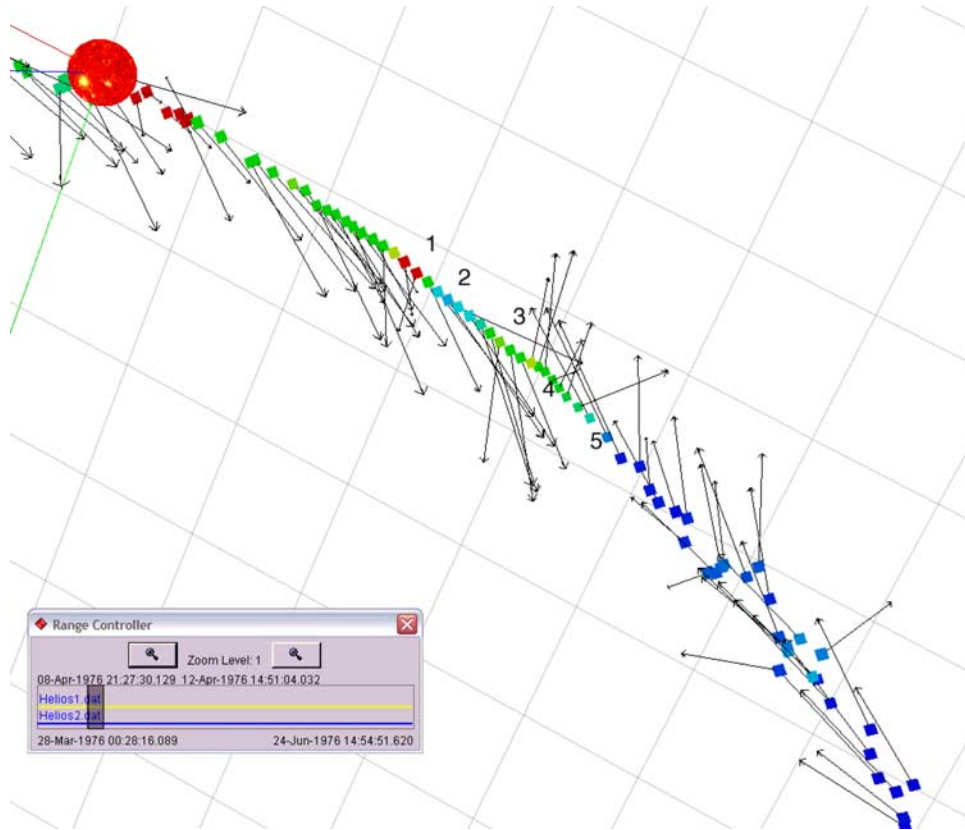


Figure 5. A three-dimensional view of a subset of the data in Figure 3 showing the magnetic field vectors, the density (rainbow colors, red high) and speed (size of glyph). The grid is an x-y plane in the ecliptic with 0.1 AU spacing between lines. The view is nearly from the North. The data were observed on days 99 (8 April) to 103 (12 April) of 1976.

again the field is nearly tangential at that point. In this case the origin of the tangential fields is not clear, but given the consistency for different rotations, the origin is probably in persistent structures at the Sun. Overall, there is a remarkably detailed correspondence between the fields seen three solar rotations distant in time. This is summarized by the numbered regions on the figures: (1) high density and tangential field, (2) lower density and more radial field, (3) more tangential presector fields, (4) postsector tangential fields, and (5) a return to highly radial fields. This correspondence also lends further credence to the suggestion the sector region itself has dynamically evolved as the plasma moved from 0.3 to 1 AU from the Sun.

[13] Returning to Figure 3, the plasma variables give us further information. First, note that on either side of the HCS the parameters are quite different. Throughout the slow wind region, but especially on the sunward (later in time) side, the normalized density is anticorrelated with the magnetic field and temperature, indicative of pressure balance structures. The properties of the near-Sun side are much more variable, the density is higher, and (not shown here; see *Goldstein et al.* [1995]) the region is much less Alfvénic than the other side as given by correlations between fluctuating velocity and magnetic field. The anti-sunward side of the transition (to the left in the figure) is very like the nearby fast wind in its Alfvénicity and entropy. All these features strongly support the conclusion that the plasma either side of the current sheet comes from different

regions, which would be in agreement with an origin near the edges of coronal holes either side of the streamer belt [*Neugebauer et al.*, 2002]. Moreover, the anticorrelation of temperature and density leads to a strong variability in the entropy on the sunward side of the transition.

[14] Compression, rarefaction, and shear, the primary dynamical processes affecting the plasma, will not change entropy until shocks form, and shocks are rare this close to the Sun. This means the most likely source of the entropy variations is differences in the properties of the originating regions for the wind near the Sun. Turning to Figure 4, we see that the variability in the entropy and other quantities is less, again indicative of dynamical processes such as, perhaps, a mixing of nearby regions or heat conduction. More detailed studies and simulations will be needed to determine exactly what process is occurring. We note that as seen in Figure 2, all regions have increasing entropy with increasing distance from the Sun, and that in this regard slow and fast wind regions are comparable. This has often been interpreted as a turbulent heating of the plasma, although it is rarely noted that the slow wind is heated as well. It may be that the same processes that are responsible for the small-scale heating (such as shear; e.g., *Tu* [1988]; *Roberts et al.* [1987b]; *Tu and Marsch* [1995]) also generate a deformation of the plasma sheet on a large scale [e.g., *Suess and Hildner*, 1985]. Note that compressions and deformations due to large-scale stream interaction [e.g., *Pizzo*, 1991] will change the relative locations of such

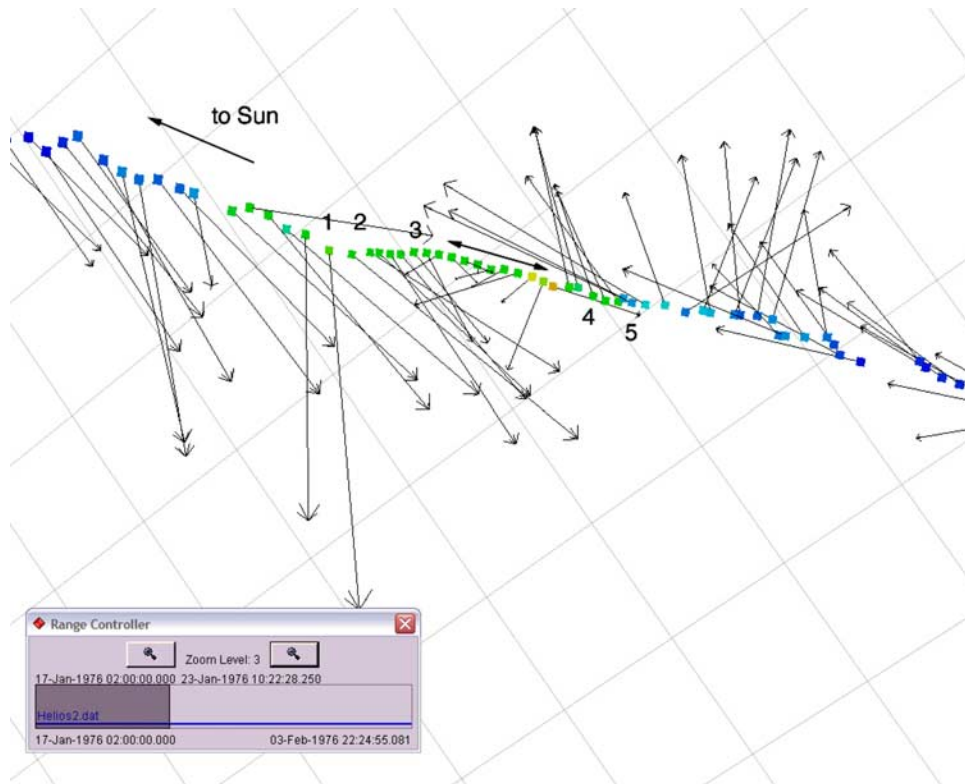


Figure 6. A three-dimensional view of subset of the data in Figure 4 showing the magnetic field vectors, the density (rainbow colors, red high) and speed (size of glyph). The Sun is off the figure to the left and the grid is as in Figure 5 with the sector crossing very near 1 AU. The data are from days 17 (17 January) to 23 (23 January) of 1976.

things as stream interfaces and sector boundaries, but they will not increase the complexity of the sector boundary crossings; the latter requires further deformations that could be due to such things as streaming instabilities.

[15] The observations discussed so far were at solar minimum when more simple transitions might be expected because the Sun is less active. Figure 7 shows a pass of Helios 1 from 0.3 AU to 1 AU and back during near solar maximum in 1980–1981. Again, it is apparent to the eye that simple transitions are more likely near the Sun, but in general there are fewer simple transitions. Note also that the transitions can be complex in the near region as seen, for example, in the first days shown on the plot. These regions may well have been produced by complex magnetic configurations near the Sun, as suggested in many detailed studies by Crooker and coworkers. There is no organized stream structure, so it is not possible to follow a simple corotating region. Statistically, using data around the solar minimum (all 1976 data from Helios 1 and Helios 2), 58% of the transitions in the near region and 27% of the transitions in the far region are simple. Around the solar maximum (1980–1981 Helios 1), 33% of the transitions in the near region and 14% of the transitions in the far region are simple. In both cases there are slightly more than twice as many simple transitions in the near region than the far region, supporting dynamical evolution. The difference between solar minimum and maximum may be due to either greater complexity in the source regions or to stronger dynamical effects, but this analysis cannot distinguish these alternatives. It is well known that the affect of the solar

cycle on magnetic structure is more dramatic over the poles of the Sun. Although there is statistical agreement with the Parker spiral predictions [Smith *et al.*, 2001], the deviations from the ideal Parker angles are much greater at solar maximum [Forsyth *et al.*, 2001]. We leave the detailed study of the polar regions for later work.

[16] Typically, at a HCS crossing there is a slow wind which is surrounded by a fast wind. However, there are some cases in which the crossing of the HCS is not clearly associated with a typical streamer belt region and there is no fast wind present. Figure 8 gives an example of a fairly constant solar wind speed over a very long period including the HCS. In this region (near day 119) the normalized density and the entropy are also fairly constant, and the fluctuations are as Alfvénic as in any high-speed wind [Roberts *et al.*, 1987b]. Except for a few peaks, the magnetic field is fairly constant also. In this case the reverse transition occurs at the time of a transient solar wind speed increase that drives a compression region (around day 133 and associated with an Alfvénicity decrease) and is more complex. The difference in the transitions may indicate the role of dynamical evolution, although the complex entropy at the time of the second transition is indicative of a complex source region as well.

[17] Finally, we note a possible complication of the interpretation of the data as we have presented it. In the near region of the spacecraft's orbit the latitude is changing much more rapidly than elsewhere in the orbit. If the majority of the simple transitions occur where the latitude is rapidly changing, then perhaps the orbit is effecting the

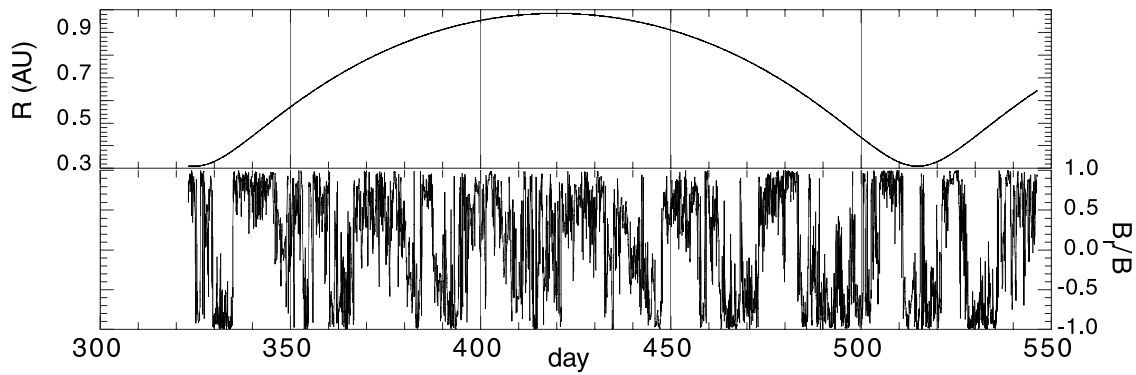


Figure 7. Data from Helios 1, 1980–1981 showing the higher complexity of HCS transitions near the time of solar maximum.

results. However, if a large number occur outside of this region, then the measured complexity is real. There are many instances in the data where simple structures are seen outside of the region of rapid latitude change. Figure 8 shows a typical example of this. The transition around day

139 is during a rapid latitude change. Around days 120 and 172 there are simple transitions which clearly lie outside of the region of rapid latitude change. This is consistent with the rest of the data, which helps support the validity of simple transitions and implies more generally that the

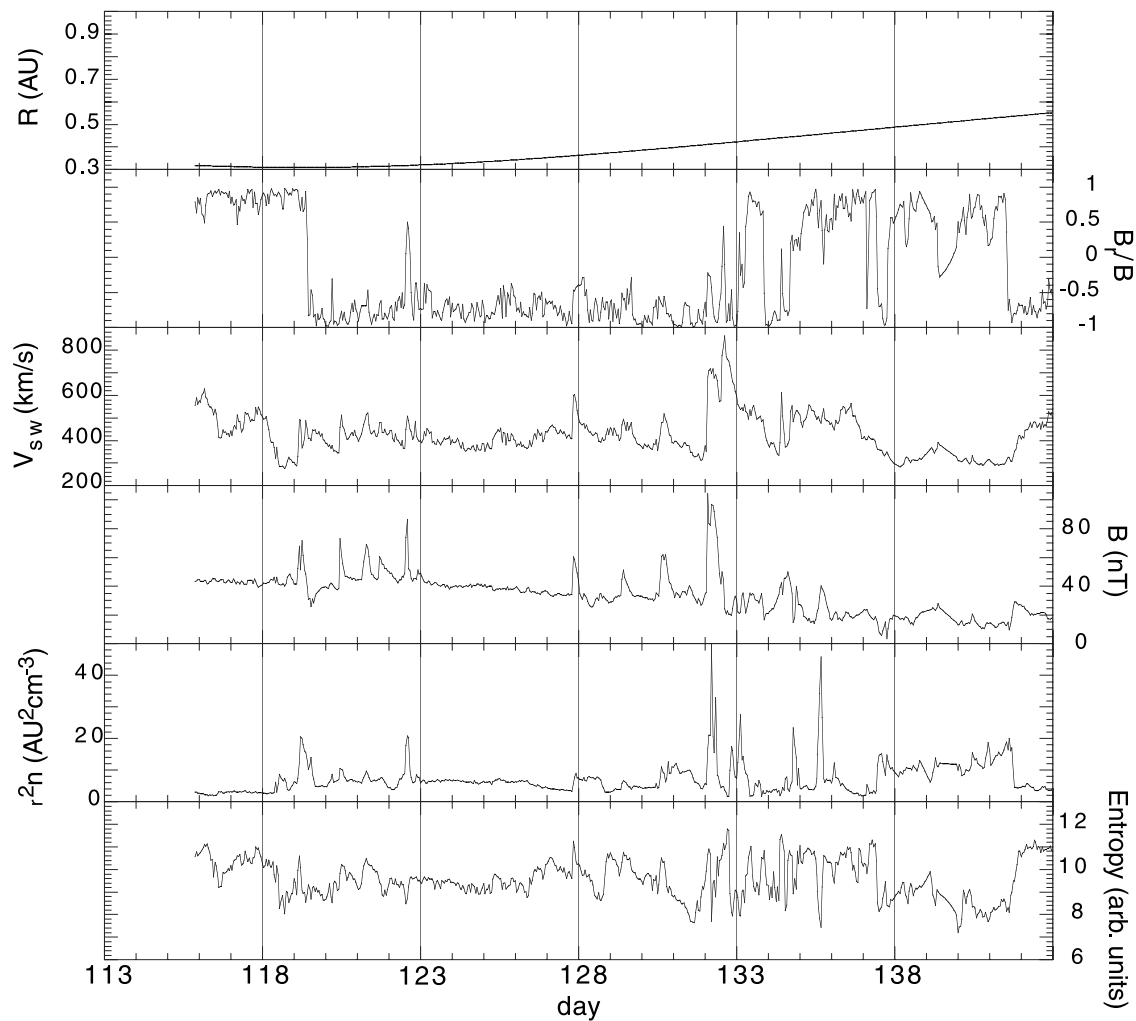


Figure 8. An example of a current sheet crossing occurring in a region of fairly constant solar wind speed, from Helios 1 1978. Near day 119 a simple transition occurs and the solar wind speed remains constant at about 440 km/s.

changing spacecraft latitude does not influence the nature of the HCS crossings.

4. Conclusions

[18] We thus find evidence for dynamical evolution of the HCS with radial distance. For example, HCS crossings tend to increase in their complexity with increasing heliocentric distance. This observation implies that the HCS becomes distorted dynamically farther from the Sun. There are cases where complexity in the HCS crossing is seen close to the Sun, and here the complexity may be of solar or lower coronal origin. However, these cases occur far less frequently than simple HCS crossings within 0.5 AU of the Sun. Complex HCS crossings are more likely near the Sun as solar activity increases, but the increasing complexity with distance from the Sun is seen throughout the solar cycle.

[19] Anticorrelations between the normalized density and the temperature at the HCS crossings coupled with differences in the entropy on either side of the HCS especially and solar minimum indicate that the plasma in either region does not have the same origin. This supports the view [e.g., Gosling *et al.*, 1981; Neugebauer *et al.*, 2002] that the plasma on the two sides of the streamer belt comes from often very different regions located either side of the helmet streamer at the base of the slow wind flow. The strong filamentary entropy structure implies the origin of the filamentation is in initial conditions near the Sun, consistent with coronal observations of highly striated structures. Smoother entropy profiles with increasing heliocentric distance indicate dynamical evolution, consistent with the increasing complexity of the HCS.

[20] Striated magnetic tubes may contain strong flow speed differences near the Sun. These could be at least in part responsible for the evolution of streamer belt and HCS. Shear flows have been suggested as the origin of such evolution by Suess and Hildner [1985]. The shears could also be responsible for the enhanced turbulent evolution seen near the current sheet regions near solar minimum [Grappin *et al.*, 1990; Marsch and Tu, 1990; Roberts *et al.*, 1987a, 1987b]. Although the strongest shears would probably have been eliminated by the dynamical evolution, it is still worth investigating the detailed correlation of shear with the evolution seen in this study; the new visualization methods used here will be of help also. It is interesting to note that the average entropy in the streamer belt increases by about the same factor as in the surrounding high-speed streams indicating that this region is heated substantially. Compression regions are not preferentially heated in the inner heliosphere; the heating is probably turbulent.

[21] The results here shed some light on the studies mentioned in section 1. In particular, we have shown that it is likely that both dynamical evolution and complex structures near the Sun play a significant role in the complexities of the HCS/streamer belt region. The evolution with distance we see is a natural precursor to that observed in the outer heliosphere, and the highly structured regions near 0.3 AU along with the entropy signatures are consistent with complex structure originating on the Sun. The complex transitions seen near 0.3 AU may, of course, have been dynamically generated closer to the Sun; a solar orbiter or probe would resolve this question. Simulations of the

heliosphere that allow waves, structures, and flows in the boundary conditions [Goldstein *et al.*, 1995; Roberts *et al.*, 2003], which have already demonstrated highly complex HCS fields given relatively simple boundary conditions, should help us with the dynamical evolution aspect of the problem. The intrinsically structured regions will be best studied by a combination of solar and in situ observations combined with simulations [e.g., Riley *et al.*, 2003; Usmanov and Goldstein, 2003].

[22] **Acknowledgments.** This work was supported, in part, by NASA Supporting Research and Technology grants to the Goddard Space Flight Center. We also thank the AISR Program and Joe Bredekamp for support for the development of ViSBARD. P. Keiter was supported by the DoE Plasma Physics Junior Faculty program during this work. The data were all retrieved from the NSSDC, and we acknowledge the many people responsible for the provision, reduction, and preparation of those data sets.

[23] Shadia Rifai Habbal thanks Richard Woo and Roberto Bruno for their assistance in evaluating this paper.

References

- Bavassano, B., R. Woo, and R. Bruno (1997), Heliospheric plasma sheet and coronal streamers, *Geophys. Res. Lett.*, **24**, 1655.
- Behannon, K. W., L. F. Burlaga, J. T. Hoeksema, and L. W. Klein (1989), Spatial variation and evolution of heliospheric sector structure, *J. Geophys. Res.*, **94**, 1245.
- Burlaga, L. F., and N. F. Ness (1993), Large-scale distant heliospheric magnetic field: Voyager-1 and Voyager-2 observations from 1986 through 1989, *J. Geophys. Res.*, **98**, 17,451.
- Burlaga, L. F., N. F. Ness, and J. D. Richardson (2003), Sectors in the distant heliosphere: Voyager 1 and 2 observations from 1999 through 2002 between 57 and 83 AU, *J. Geophys. Res.*, **108**(A10), 8028, doi:10.1029/2003JA009870.
- Crooker, N. U. (1999), Heliospheric current sheet structure, in *Solar Wind Nine*, edited by S. Habbal *et al.*, *AIP Conf. Proc.*, **471**, 93.
- Crooker, N. U. (2003), Heliospheric plasma and current sheet structure, in *Solar Wind Ten*, edited by M. Velli, R. Bruno, and F. Malara, *AIP Conf. Proc.*, **679**, 93.
- Crooker, N. U., M. E. Burton, G. L. Siscoe, S. W. Kahler, J. T. Gosling, and E. J. Smith (1996), Solar wind streamer belt structure, *J. Geophys. Res.*, **101**, 24,331.
- Forsyth, R. J., A. Balogh, and E. J. Smith (2001), Latitudinal variation of the underlying heliospheric magnetic field direction: Comparison of the Ulysses first and second orbits, *Space Sci. Rev.*, **97**, 161.
- Goldstein, M. L., D. A. Roberts, and W. H. Matthaeus (1995), Magnetohydrodynamic turbulence in the solar wind, *Annu. Rev. Astron. Astrophys.*, **28**, 283.
- Gosling, J. T., G. Borini, J. R. Asbridge, S. J. Bame, W. C. Feldman, and R. T. Hansen (1981), Coronal streamers in the solar wind At 1-AU, *J. Geophys. Res.*, **86**, 5438.
- Grappin, R., A. Mangeney, and E. Marsch (1990), On the origin of solar wind MHD turbulence: Helios data revisited, *J. Geophys. Res.*, **95**, 8197.
- Marsch, E., and C.-Y. Tu (1990), On the radial evolution of MHD turbulence in the inner heliosphere, *J. Geophys. Res.*, **95**, 8211.
- Neugebauer, M., P. C. Liewer, E. J. Smith, R. M. Skoug, and T. H. Zurbuchen (2002), Sources of the solar wind at solar activity maximum, *J. Geophys. Res.*, **107**(A12), 1488, doi:10.1029/2001JA000306.
- Pizzo, V. J. (1991), The evolution of corotating stream fronts near the ecliptic plane in the inner solar system: 2. Three-dimensional tilted-dipole fronts, *J. Geophys. Res.*, **96**, 5405.
- Riley, P., J. A. Linker, Z. Mikic, D. Odstrcil, T. H. Zurbuchen, D. Lario, and R. P. Lepping (2003), Using an MHD simulation to interpret the global context of a coronal mass ejection observed by two spacecraft, *J. Geophys. Res.*, **108**(A7), 1272, doi:10.1029/2002JA009760.
- Roberts, D. A., L. W. Klein, M. L. Goldstein, and W. H. Matthaeus (1987a), The nature and evolution of magnetohydrodynamic fluctuations in the solar wind: Voyager observations, *J. Geophys. Res.*, **92**, 11,021.
- Roberts, D. A., M. L. Goldstein, L. W. Klein, and W. H. Matthaeus (1987b), Origin and evolution of fluctuations in the solar wind: Helios observations and Helios-Voyager comparisons, *J. Geophys. Res.*, **92**, 12,023.
- Roberts, D. A., M. L. Goldstein, and A. Deane (2003), Three-dimensional MHD simulation of solar wind structure, in *Solar Wind Ten*, edited by M. Velli, R. Bruno, and F. Malara, *AIP Conf. Proc.*, **679**, 133.
- Smith, E. J. (2001), The heliospheric current sheet, *J. Geophys. Res.*, **106**, 15,819.

- Suess, S. T., and E. Hildner (1985), Deformation of the heliospheric current sheet, *J. Geophys. Res.*, *90*, 9461.
- Szabo, A., R. P. Lepping, and D. E. Larson (1999), The heliospheric current sheet on small scale, in *Solar Wind Nine*, edited by S. Habbal et al., *AIP Conf. Proc.*, *679*, 589.
- Thieme, K. M., E. Marsch, and R. Schwenn (1990), Spatial structures in high-speed streams as signatures of fine structures in coronal holes, *Ann. Geophys.*, *8*, 713.
- Tu, C.-Y. (1988), The damping of interplanetary Alfvénic fluctuations and the heating of the solar wind, *J. Geophys. Res.*, *93*, 7.
- Tu, C. Y., and E. Marsch (1995), MHD structures, waves and turbulence in the solar wind: Observations and theories, *Sp. Sci. Rev.*, *73*, 1.
- Usmanov, A. V., and M. L. Goldstein (2003), A tilted-dipole MHD model of the solar corona and solar wind, *J. Geophys. Res.*, *108*(A9), 1354, doi:10.1029/2002JA009777.
- Winterhalter, D., E. J. Smith, M. E. Burton, N. Murphy, and D. J. McComas (1994), The heliospheric plasma sheet, *J. Geophys. Res.*, *99*, 6667.
- Woo, R., J. W. Armstrong, and P. R. Gazis (1995), Doppler scintillation measurements of the heliospheric current sheet and coronal streamers close to the Sun, *Space Sci. Rev.*, *72*, 223.

M. L. Goldstein and D. A. Roberts, NASA Goddard Space Flight Center, Laboratory for Solar and Space Physics, Code 612.2, Greenbelt, MD 20771, USA. (melvyn.l.goldstein@nasa.gov; aaron.roberts@gsfc.nasa.gov)

P. A. Keiter, P-24 Plasma Physics, P. O. Box 1663, MS E-526, Los Alamos National Laboratory, Los Alamos, NM 87545, USA. (pkeiter@lanl.gov)